

Supporting Information for

Cadmium Isotopes Analysis of Environmental Samples with High Organic Matter by Dry Ashing Method under Wet Plasma Conditions

Xian Wu^{1, 2}, Zeyu Wang^{1, 3}, Guangyi Sun^{1, *}, Yu Lin^{1, 2}, Xuewu Fu^{1, *}, Yang Tang¹, Xinbin Feng^{1,}
²

¹ State Key Laboratory of Environmental Geochemistry, Institute of Geochemistry, Chinese Academy of Sciences, Guiyang 550081, China

² University of Chinese Academy of Sciences, Beijing 100049, China

³ College of Eco-Environmental Engineering, Guizhou Minzu University, Guiyang, Guizhou 550025, China

* Corresponding authors: Guangyi Sun (sunguangyi@mail.gyig.ac.cn) and Xuewu Fu (fuxuewu@mail.gyig.ac.cn)

This supporting information includes 3 equations, 5 figures and 2 tables.

Chemical reaction equations(S1-S3). Possible reactions of Cd compounds during dry ashing

Figure S1. Schematic diagram of dry ashing heating procedure

Figure S2. Relationship between ΔCd and Zr content. (ΔCd is the difference value between the Cd content measured by ICP-MS and GF-AAS, respectively.)

Figure S3. Comparison photo of non-dry-ashed sample and dry ashed sample(Left: non-dry-ashed sample, right: dry ashed sample ;take GSD-11 as an example)

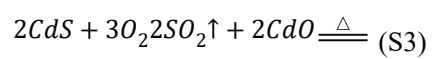
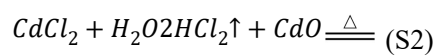
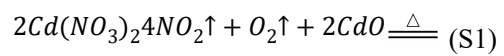
Figure S4. Box plot of purification recovery distribution for dry-ashed standard samples

Figure S5. Comparison of Cd isotopic compositions of dry-ashed samples with different purification recovery ranges, reference values: GSS-5 from Peng *et al.* (2021)¹; GSD-12 from Lu *et al.* (2021)²; NIST SRM 2711a and GSS-4 from Tan *et al.* (2020)³; BCR-482 from Borovička *et al.* (2020)⁴

Table S1. The reference material information

Table S2. Trace elements in QMA filter membranes and sediments

**Chemical reaction equations(S1-3). Possible reactions of Cd compounds during
dry ashing**



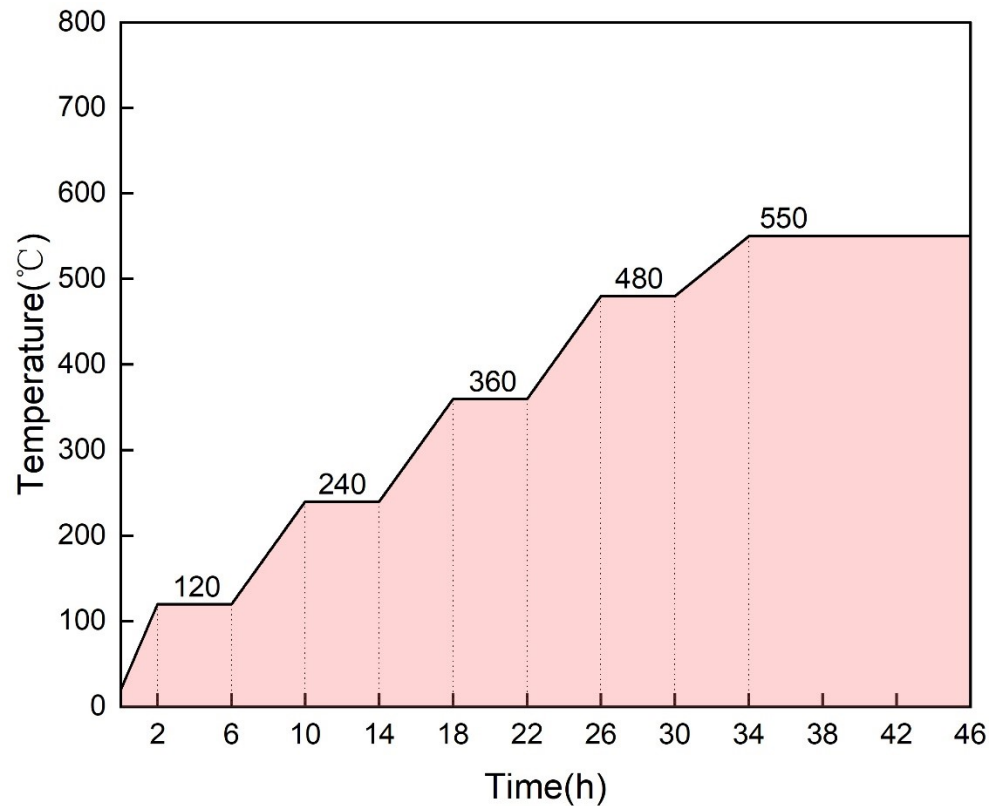


Figure S1. Schematic diagram of dry ashing heating procedure

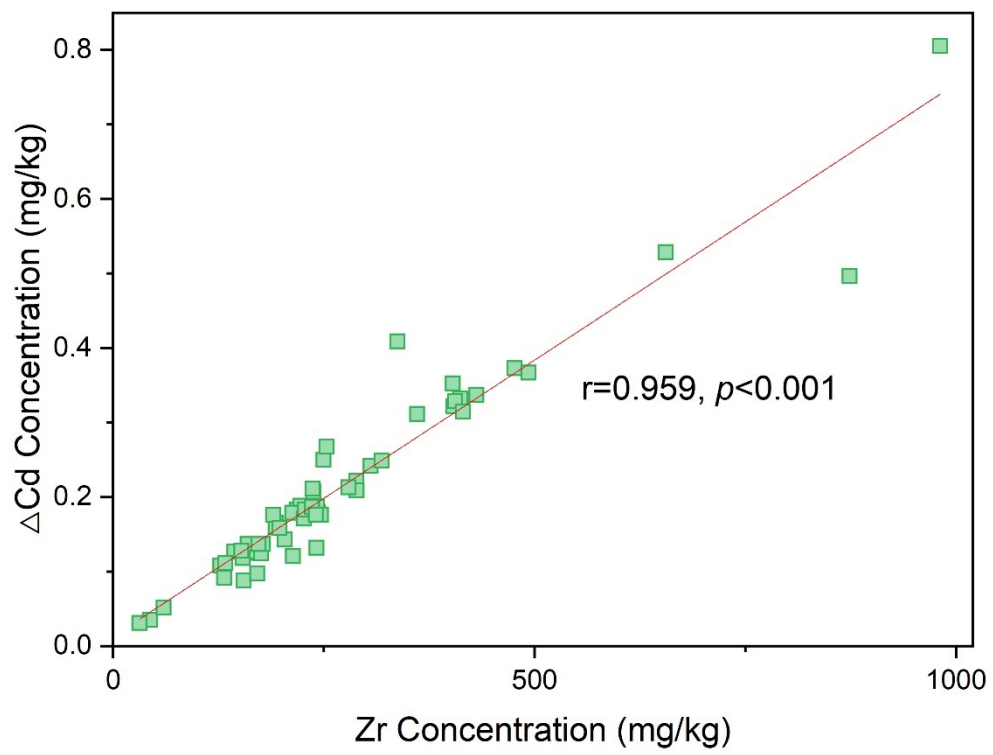
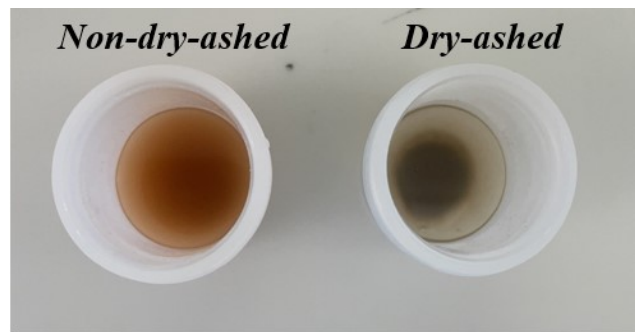
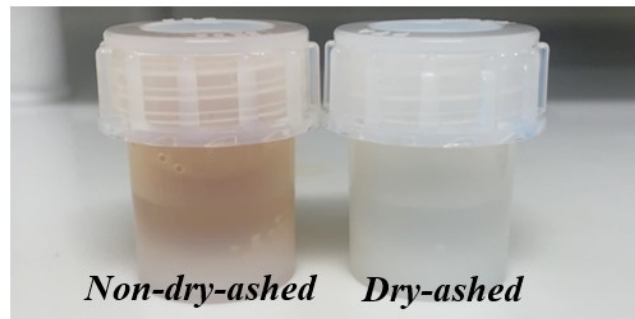


Figure S2. Relationship between ΔCd and Zr Content. (ΔCd is the difference value between the Cd content measured by ICP-MS and GF-AAS, respectively.).



Primary stage



Resolution stage

Figure S3. Comparison photo of non-dry-ashed sample and dry ashed sample(Left: non-dry-ashed sample, right: dry ashed sample ;take GSD-11 as an example)

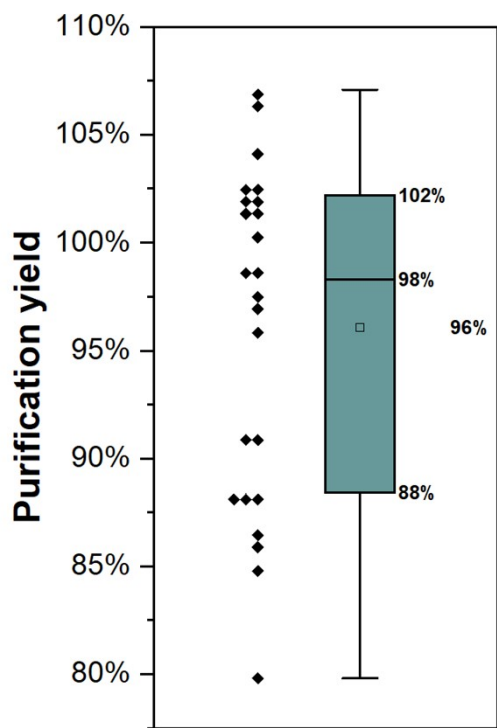


Figure S4. Box plot of purification recovery distribution for dry-ashed standard samples

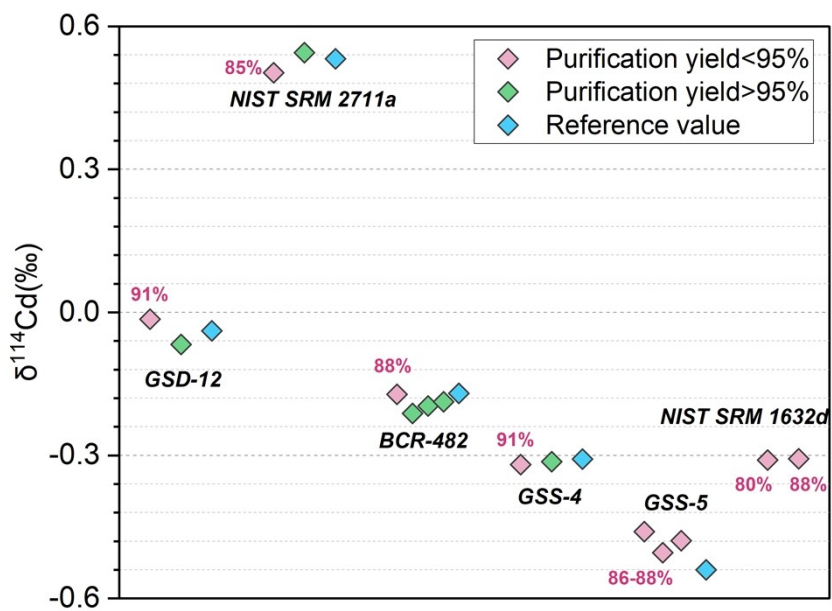


Figure S5. Comparison of Cd isotopic compositions of dry-ashed samples with different purification recovery ranges, reference values: GSS-5 from Peng *et al.* (2021)¹; GSD-12 from Lu *et al.* (2021)²; NIST SRM 2711a and GSS-4 from Tan *et al.* (2020)³; BCR-482 from Borovička *et al.* (2020)⁴

Table S1. The reference material information

Sample name	Concentration ($\mu\text{g g}^{-1}$)	Sample description
NIST SRM 2711a	54.1 ± 0.5	Montana II Soil
GSS- 4(GBW07404)	0.35 ± 0.08	Limestone weathered soil in Yishan, Guangxi Province, China
GSS- 5(GBW07405)	0.45 ± 0.09	Yellow-red soil in Qibaoshan skarn copper polymetallic ore district, Hunan Province, China
GSD- 11(GBW07311)	2.3 ± 0.2	River sediment from Shizhuyuan polymetallic mining area, Hunan Province, China
GSD- 12(GBW07312)	4.0 ± 0.3	River sediment from Yangchun polymetallic mining area in Guangdong Province, China
BCR-482	$0.50 \pm 0.02^*$	Lichen
GSB- 16(GBW10025)	0.37 ± 0.03	Spirulina platensis
GSB- 29(GBW10051)	1.00 ± 0.02	Pork liver
NIST SRM 1632d	0.08 ± 0.01	Bituminous Coal

*This value is obtained from long-term observations in this study and is consistent with Kłos *et al.*(2012)⁵.

Table S2. Trace elements in QMA filter membranes and sediments

Sample	Units	Ga	Zr	Mo	Cd (ICP-MS)	Cd (GF-AAS)
QMA Fliter-1	ng dm ⁻²	185.9	7612.0	38497.1	44.6	2.1
QMA Fliter-2	ng dm ⁻²	187.6	7608.2	38574.7	42.3	1.6
QMA Fliter-3	ng dm ⁻²	219.4	9301.9	45567.3	52.6	3.3
NSS-1	µg g ⁻¹	7.531	127.361	0.145	0.111	0.003
NSS-2	µg g ⁻¹	23.703	411.712	1.045	0.356	0.023
NSS-3	µg g ⁻¹	17.766	655.734	0.562	0.575	0.047
NSS-4	µg g ⁻¹	24.524	193.485	0.940	0.234	0.068
NSS-5	µg g ⁻¹	26.032	172.931	1.349	0.154	0.029
NSS-7	µg g ⁻¹	10.902	143.761	0.556	0.138	0.011
NSS-8	µg g ⁻¹	30.276	165.820	1.988	0.359	0.233
NSS-9	µg g ⁻¹	2.254	43.606	0.211	0.038	0.003
NSS-10	µg g ⁻¹	20.114	237.393	0.676	0.247	0.040
NSS-11	µg g ⁻¹	24.460	430.924	0.901	0.367	0.030
NSS-12	µg g ⁻¹	18.165	981.180	0.374	0.827	0.022
NSS-13	µg g ⁻¹	23.920	492.757	0.776	0.440	0.073
NSS-14	µg g ⁻¹	12.219	131.791	0.326	0.111	0.020
NSS-15	µg g ⁻¹	14.182	403.767	0.381	0.325	0.003
NSS-16	µg g ⁻¹	14.308	192.838	0.472	0.168	0.009
NSS-17	µg g ⁻¹	11.395	476.474	0.247	0.376	0.003
NSS-18	µg g ⁻¹	7.366	154.942	0.337	0.159	0.072
NSS-19	µg g ⁻¹	1.875	31.189	0.129	0.034	0.003
NSS-20	µg g ⁻¹	1.677	59.854	0.192	0.055	0.003
NSS-21	µg g ⁻¹	17.346	217.790	0.730	0.234	0.051
NSS-22	µg g ⁻¹	18.501	405.464	0.872	0.401	0.073
NSS-23	µg g ⁻¹	18.687	305.560	0.848	0.310	0.068
NSS-24	µg g ⁻¹	27.180	222.157	1.424	0.288	0.099
NSS-25	µg g ⁻¹	29.441	175.265	1.190	0.260	0.136
NSS-26	µg g ⁻¹	25.928	241.537	1.034	0.629	0.497
NSS-27	µg g ⁻¹	23.911	288.346	1.302	0.622	0.401
NSS-28	µg g ⁻¹	25.443	230.995	0.862	0.517	0.334
NSS-29	µg g ⁻¹	23.380	212.328	0.703	0.205	0.027
NSS-30	µg g ⁻¹	24.925	242.475	1.070	0.333	0.153
NSS-31	µg g ⁻¹	25.486	203.949	0.834	0.187	0.044
NSS-32	µg g ⁻¹	27.947	241.632	0.985	0.511	0.324
NSS-33	µg g ⁻¹	26.483	189.939	1.234	0.553	0.377
NSS-34	µg g ⁻¹	26.526	236.736	1.081	0.787	0.577

NSS-35	$\mu\text{g g}^{-1}$	27.760	226.018	1.130	0.628	0.458
NSS-36	$\mu\text{g g}^{-1}$	24.660	360.644	1.026	0.558	0.247
NSS-37	$\mu\text{g g}^{-1}$	35.862	171.136	1.835	0.822	0.725
NSS-38	$\mu\text{g g}^{-1}$	30.223	402.882	2.176	0.804	0.452
NSS-39	$\mu\text{g g}^{-1}$	33.786	249.750	2.911	1.422	1.172
NSS-41	$\mu\text{g g}^{-1}$	26.454	337.488	1.102	0.646	0.237
NSS-40	$\mu\text{g g}^{-1}$	18.338	873.562	0.579	0.901	0.405
NSS-42	$\mu\text{g g}^{-1}$	22.158	253.617	1.221	0.844	0.577
NSS-43	$\mu\text{g g}^{-1}$	24.717	227.587	1.232	0.769	0.586
NSS-44	$\mu\text{g g}^{-1}$	21.627	415.018	0.990	1.628	1.313
NSS-45	$\mu\text{g g}^{-1}$	27.880	236.151	1.124	0.272	0.086
NSS-46	$\mu\text{g g}^{-1}$	30.104	246.683	1.278	0.374	0.198
NSS-47	$\mu\text{g g}^{-1}$	21.587	289.177	1.103	1.407	1.198
NSS-48	$\mu\text{g g}^{-1}$	26.979	159.507	1.485	0.187	0.050
NSS-49	$\mu\text{g g}^{-1}$	26.453	177.993	1.230	0.182	0.046
NSS-50	$\mu\text{g g}^{-1}$	22.670	279.542	1.079	0.275	0.062
NSS-51	$\mu\text{g g}^{-1}$	27.625	172.854	1.334	0.161	0.024
NSS-52	$\mu\text{g g}^{-1}$	28.716	132.789	1.492	0.302	0.191
NSS-53	$\mu\text{g g}^{-1}$	24.022	153.957	2.093	0.177	0.059
NSS-54	$\mu\text{g g}^{-1}$	21.582	240.518	1.626	0.331	0.155
NSS-55	$\mu\text{g g}^{-1}$	12.966	318.590	0.533	0.273	0.024
NSS-56	$\mu\text{g g}^{-1}$	19.484	197.278	0.859	0.181	0.022

References

- 1 H. Peng, D. He, R. Guo, X. Liu, N. S. Belshaw, H. Zheng, S. Hu and Z. Zhu, *J. Anal. At. Spectrom.*, 2021, **36**, 390–398.
- 2 Z. Lu, J.-M. Zhu, D. Tan, X. Wang and Z. Zheng, *Geostandards and Geoanalytical Research*, 2021, **45**, 565–581.
- 3 D. Tan, J.-M. Zhu, X. Wang, G. Han, Z. Lu and W. Xu, *J. Anal. At. Spectrom.*, 2020, **35**, 713–727.
- 4 J. Borovička, L. Ackerman and J. Rejšek, *Talanta*, 2021, **221**, 121389.
- 5 A. Kłos, M. Czora, M. Rajfur and M. Waclawek, *Water Air Soil Pollut.*, 2012, **223**, 1829–1836.